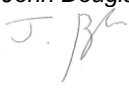# Azimuthal dependence of seismic wave attenuation in Central Europe

Work package 3   Ground motion

AUTHORS		REVIEW		APPROVAL	
Name	Date	Name	Date	Name	Date
Jiří Málek Jiří Vackář	2019/09/20	*John Douglas* 2020/04/13 *Ian Main* 2020/04/14		*Jiří Füzér* **Public access**	2020/04/17

Document history

DATE	VERSION	COMMENTS
2020/04/08	1	*Final version of original manuscript (including revisions proposed by reviewers from the SIGMA-2 Scientific Committee)*

Executive summary

The main goal is to describe azimuthal dependence of attenuation of seismic waves in the Bohemian Massif and its vicinity (Central Europe). Macroseismic studies of various historical earthquakes with epicenters in the Central Europe region have shown a significant elongation of isoseismal lines in some directions (Zátopek, 1948). Recently, this phenomenon was confirmed on the basis of instrumental records of two moderate-size earthquakes in the Vienna Basin (Málek et al., 2017). It has been found that the peak ground velocity amplitudes (*PGV*) and peak ground acceleration amplitudes (*PGA*) at comparable epicentral distances but different azimuths may vary by as much as one order of magnitude. An inspection of the individual seismograms suggests that the phenomenon is associated mainly with the propagation of high-frequency S waves. Significant differences in frequency content of the seismic waves radiated to different azimuths are also demonstrated.

Within the scope of SIGMA-2, we have investigated the azimuthal dependence for several moderate-size earthquakes in Central Europe with moment magnitudes between 2.3 and 3.8. We selected 9 earthquakes from 7 seismic epicentral zones from the years 2012 to 2018, which represent the strongest events in those zones for the last decade. The number of seismic stations in the region under investigation has been increasing (both permanent and temporary). It enables us to observe the attenuation of seismic waves directly from the measured seismograms. The results show that the *PGV* and *PGA* depends strongly on the azimuth of wave propagation for some earthquakes. The azimuthal dependence has not been considered yet in the evaluation of seismic hazard for the Temelín and Dukovany nuclear power plants which are situated in the Bohemian Massif.

Azimuthal dependence of amplitudes is not considered in the standard methodology of PSHA. We recommend its modification in order to estimate the truly site-specific seismic hazard.

Contents

Introduction

The Bohemian Massif in Central Europe represents an intraplate region with weak but not negligible seismicity. Two nuclear power plants (NPPs) are situated there and several other NPPs are in neighboring countries. Two reactors (each of 1055 MWe) are in operation at Temelín NPP and four reactors (each of 510 MWe) are in operation at Dukovany NPP. There are plans to extend one or both of these power plants in the near future. The last Probabilistic Seismic Hazard Assessment (PSHA) was performed by Málek et al., (2012) for Temelín NPP and by Málek and Prachař (2015) for Dukovany NPP. Since then, some specific features in the methodology have been identified and analyzed. One of the most important features is the fact that the most dangerous seismic source zones are situated at a relatively large distance from the sites of the nuclear power plants, more than 100 km. Therefore, the description of attenuation of seismic waves is one of the most important sources of epistemic uncertainty in PSHA for these sites. As the region reveals only weak seismicity, there are no instrumental records of strong ground motion, which could be used for site-specific assessment of seismic wave attenuation. In principle, there are two approaches to selecting the appropriate ground motion model (GMM) to describe the attenuation. The first one, which is a standard approach, is to adopt a GMM from some other region with stronger seismicity but similar geological and tectonic setting. For the Bohemian Massif, such region could be Central and East North America (CENA). For the CENA region, there are several GMMs; the most recent one is NGA-East model (Goulet et al., 2017).

The second approach is to use moderate-size instrumentally recorded earthquakes in the most important seismic zones of the region and to extrapolate the features of measured seismograms for larger magnitudes. This approach was selected in this study. The extrapolation to larger magnitudes can be done again with the help of the NGA-East model.

The advantage of the selected approach is straightforward. We can examine site-specific features of the seismic field. One of them is the azimuthal dependence of the GMM model. The azimuthal dependence has turned out to be very strong for seismic zones along the border of the Bohemian Massif. It has a strong impact on the seismic hazard of NPPs inside the Bohemian Massif. In future, it will enable us to perform truly site-specific seismic hazard computation, considering the individual GMMs for each of the seismic zones.

1. Selection of seismic events

Earthquakes in the Bohemian Massif have been instrumentally recorded since November 28, 1908, when the first seismic station in Cheb was put into operation. Bulletins of seismic events (with onset times and maximal amplitudes) are available from January 1976. At that time, only 2 stations were included in the catalog, namely Průhonice (PRU) and Kašperské hory (KHC). This was the origin of the Czech Regional Seismic Network (CRSN). The number of seismic stations in the Czech Republic has increased up to 20 permanent seismic stations operated by CRSN and several tens of other stations in local networks. Comparable numbers of stations are also in the neighboring countries. However, the digital seismic data from most of the existing seismic stations are available only for the most recent years. This was the main reason why we decided to select only the earthquakes since 2012.

The nine used events (E1 – E9) from seven source zones are listed in Table 1. We have chosen pairs of events from West Bohemia (E4 and E8) and Lubin (E6 and E9) so that we can compare the stability of the results for different events from the same zone. The location errors are small for epicenters but the depth is not well delimited for events E1, E3 and E7. However, it is clear that all events are shallow, with depth less than 15 km. Three earthquakes represent induced seismic events from mining areas: Ostrava coal mines (E5) and the Lubin copper mine (E6 and E9). Two events (E4 and E8) are from West Bohemia which is well-known for the occurrence of seismic swarms. Two events are from different

parts of the Austrian Alps (E1 and E3) and one event is from the Vienna Basin (E7). Another event is from the Little Carpathians in Slovakia (E2).

| ID	Date & time	Lat	Lon	Mw	Source zone	Stations
	UTC	N	E			
E1	2012-01-17 11:41:01.0	47.83	14.21	2.4	Kalkalpen, Austria	121
E2	2012-03-05 22:56:57.0	48.54	17.14	2.3	Malé Karpaty, Slovakia	66
E3	2014-04-17 14:59:17.0	47.60	15.49	2.9	Mürzsteger Alps, Austria	136
E4	2014-05-31 10:37:20.9	50.18	12.41	3.8	Nový Kostel, Czechia	157
E5	2014-11-14 10:44:18.4	49.90	18.40	2.3	Ostrava, Czechia	71
E6	2015-07-08 06:53:18.1	51.52	16.09	3.3	Lubin, Poland	119
E7	2016-04-25 10:28:22.9	48.08	16.14	3.4	Vienna, Austria	158
E8	2018-05-21 21:04:43.0	50.24	12.46	3.4	Nový Kostel, Czechia	151
E9	2018-07-20 03:31:30.7	51.57	16.18	3.3	Lubin, Poland	119

Table 1: Parameters of analyzed earthquakes.
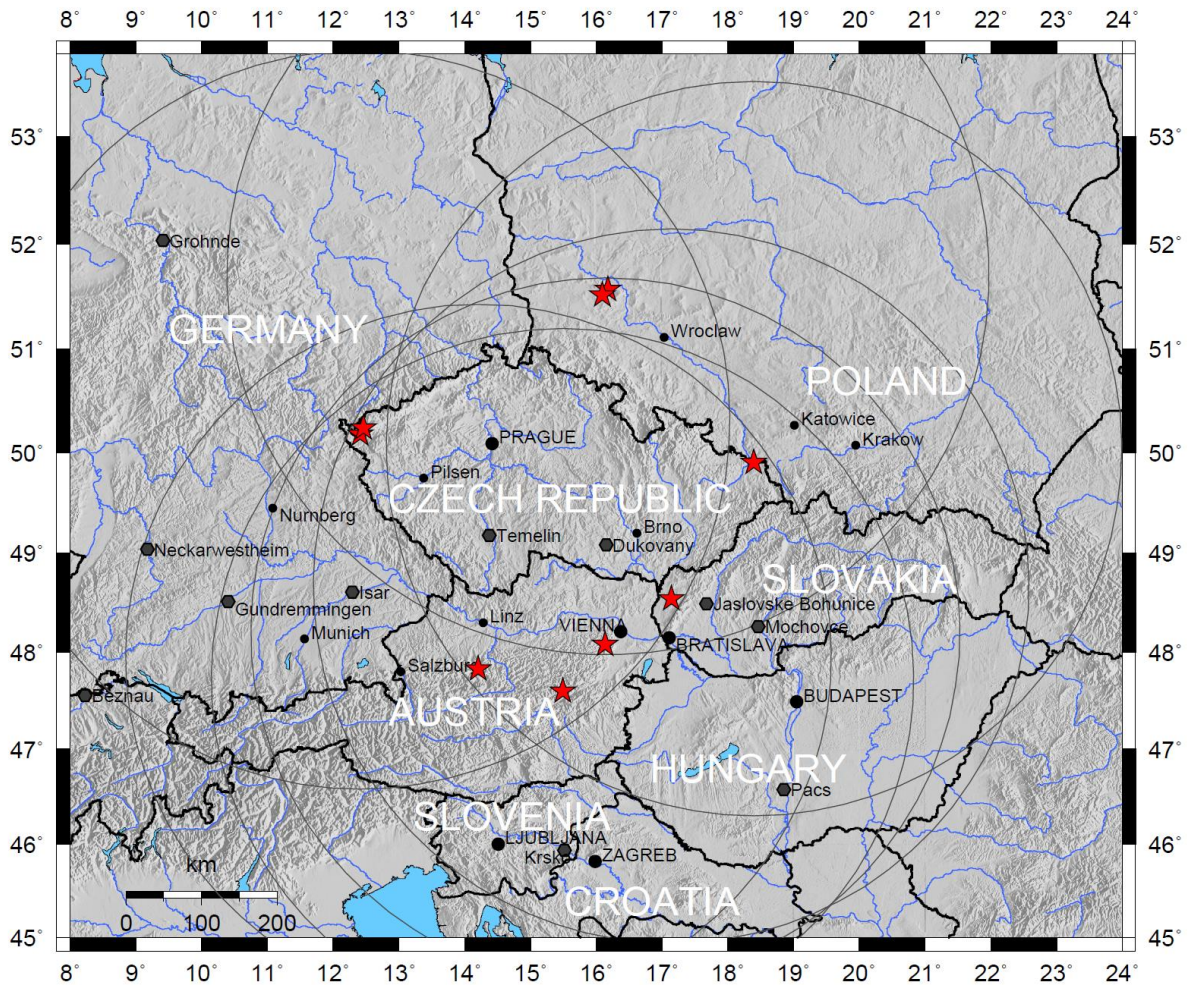
Figure 1: Selected events and the respective investigated regions within the radius of 400 km.

Catalogues provide different types of magnitudes for selected events, mainly local magnitudes. Only for E5, the moment magnitude Mw = 3.8 was published by Geofon (GFZ Potsdam). We used that value to

determine Mw for all the other events, using the vertical component of peak ground velocity (PGV-Z) in the epicentral distances from 50 to 400 km. In these epicentral distances, the effect of different hypocenter depths is small. Computed Mw magnitudes are given in Table 1. Although the estimation of Mw is very rough, it does not affect the results significantly because the method used in the present study is based on comparison of amplitudes from a single event at different stations. The selected events are shown in Fig.1. We analyzed the seismic waves up to the distance of 400 km. Although the standard radius of the investigated region around nuclear power plants is 300 km, in special cases of weak seismicity near NPPs it could be useful to extend it to 400 km. There are also several other NPPs in the investigated region: in Slovakia, Hungary and Germany.

2. Seismic stations

The quality and instrumentation of seismic stations in the region vary greatly. On the one hand, there are permanent broadband stations that are intended mainly to detect distant earthquakes and are situated at sites with low seismic noise. Unfortunately, these stations are often sampled only at 20 Hz, so they register seismic motions only up to 8 Hz. On the other hand, there are stations from local networks, which are intended to register local earthquakes. They have a high sampling frequency (100 Hz or even 250 Hz) but the sensors are often short-period (they register only the frequencies over 1 Hz) and the seismic noise is higher (as a rule). Therefore, the frequency range covered by all stations is very narrow (from 1 to 8 Hz). This problem has been solved recently, when many of the permanent stations started to provide high-frequency channels (e.g. the CRSN stations) and the sensors at local networks have been replaced with broadband ones (e.g. the local network WEBNET in West Bohemia).

In our present study, we use stations with high sampling (more than 80 Hz), both broadband and short-period ones. It reduces considerably the number of useful stations but it makes it possible to extend the range of frequencies under investigation from 1 Hz to 35 Hz, which covers the most dangerous seismic motion for nuclear power plants. We selected seismic stations with epicentral distance up to 400 km for each of events E1-E9.

3. Seismograms

The seismograms at all selected stations were inspected by seismologists on the screen. The seismograms with high seismic noise or electronic disturbances were excluded. Only 3-component seismograms are used. The original seismograms (provided by the network operators) are records of the velocity of movement, which is affected by frequency response of the sensor and is recorded with different sampling frequencies. To obtain comparable data, we corrected all seismograms for frequency characteristics of the sensor and filtered them using band-pass filter 1–35 Hz. Then we performed digital derivative to obtain accelerograms, more common in seismic hazard computations. The filtration changes the values of *PGA* and *PGV*. However, in the more distant stations (more than 50 km), the difference caused by the low-pass filter is less than 10%. This is demonstrated at the KRUC station, Fig. 2. The effect of filtering is larger for stations near the epicenter. This was one of the reasons why we restricted our study to stations within epicentral distance of 50 km. There are few stations where *PGV* is connected with surface waves. In such case, *PGV* is affected strongly by the high-pass filter at 1 Hz. Surface waves were excluded from our analyses using the above mentioned filtering.
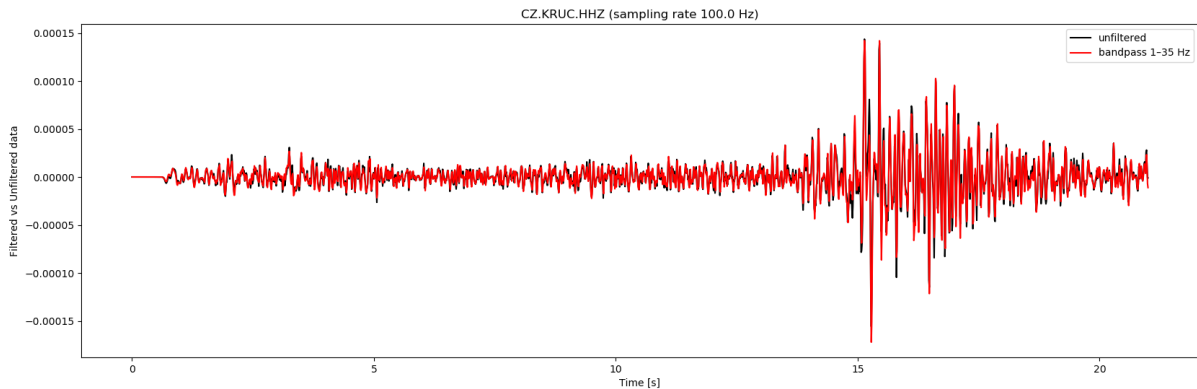
Figure 2: Seismogram at the KRUC station before (black line) and after filtering (red line)

The numbers of seismograms used for the selected earthquakes are in Tab.1. We have at least 66 selected seismograms for each earthquake. Altogether, we have at our disposal 1098 three-component accelerograms in epicentral distances up to 400 km. Out of that number, 1043 seismograms are in the interval of 50 – 400 km. The main parameters of the seismograms are listed in in Appendix 1. For each seismogram, the name of the station, epicentral distance and azimuth from the epicenter to the station is given. Peak ground acceleration *PGA* and peak ground velocity *PGV* (after filtering) at vertical component and horizontal plane are also given. The amplitude in the horizontal plane is computed as $\sqrt{N^2 + E^2}$, N and E are the components to North and East. In the last column, there is the ratio:

$$F_M = \frac{PGA_Z}{2\pi PGV_Z} \tag{1}$$

which gives us rough information about the prevailing frequency at times of peak amplitudes at vertical component Z. This parameter will be used in the next chapters to characterize the differences of frequency contents.

4. Verification of the quality of input seismograms

In many seismological applications, only the time of seismic wave onsets is used. That is why many seismological observatories are not concerned about the correct determination of amplitude. In many seismological databases, there are many errors in the signal gain. We must carefully verify the gain and repair or exclude erroneous input data.

We performed three types of tests to find the errors. In the first test, we compared PGV_Z at close stations (the distance between the stations is less than 50 km). Only stations with epicentral distance exceeding 80 km were tested. We assume that PGV_Z at such pairs of stations is comparable, their ratio should be in the interval (0.1, 10). When we found a discrepancy, we tried to contact the owner of the station and asked for a correction of the gain. In some cases, we were not successful even after such communication, so we had to exclude the station from the data set.

The second test was performed only for broadband stations. They register microseisms with prevailing frequency of 6s. It could be assumed that the amplitude of these microseisms does not vary much in the predefined time interval of 10 minutes just before the event. Again, we compared it for close stations (in this case, the distance between the stations is less than 100 km). And again, we found some suspicious stations and discussed the correctness of the gains with their providers.

The third test was made with the help of six distant earthquakes, namely Mexico 20.3.2012, M=7.3; Chile 1.4.2014, M=8.1; Nepal 25.4.2015, M=7.8; Chile 16.9.2015, M=8.3; Equador 16.4.2016 M=7.8; Fiji 19.8.2018 M=8.2. The amplitudes of Z component of P waves and S waves should be comparable at close stations. The procedure was the same as in the case of microseisms. The same data were used to characterize local conditions at the stations, see Chapter 5.

Unfortunately, the above methods do not allow us to find errors in cases where the gain differs from the right value only slightly. However, we are sure that such small errors do not affect the results of our analysis significantly.

In Figure 3, microseisms registered at broadband stations are shown for E8, as an example. The amplitudes of the microseisms are characterized as the power spectrum integrated for the frequencies 0.1–0.5 Hz.
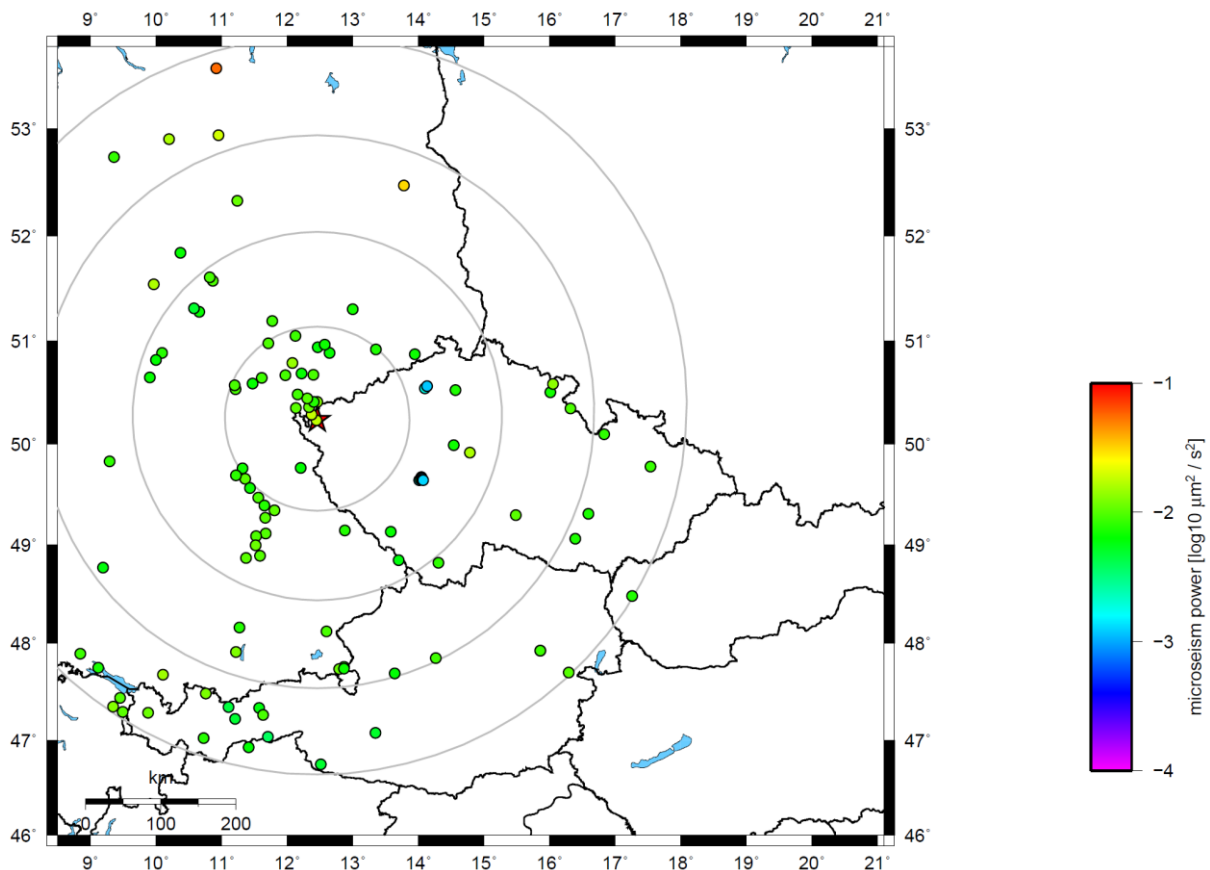

Figure 3: Amplitudes of microseisms at the broadband stations just before earthquake E8.

5. Compensation of local conditions

Ground motion at some stations can be increased by thick layers of sediments near the surface, by topography of the surface or by other local factors. These local conditions can superpose the effect of azimuthal dependence, which is the main aim of our study.

Local conditions influence all seismic waves from all seismic sources coming to the station. The amplification factor depends on the frequency of seismic waves, angle of incidence or type of the wave. We can compensate the impact of local conditions only partly. The simplest way to do it is to multiply the seismograms by constant factors that are determined for each station and for vertical and horizontal components.

To determine the factors, we can use records of P and S waves from distant earthquakes. These waves reach all stations with small incidence angles and the distance between the stations is small in comparison with epicentral distance. Therefore, their amplitude should be the same if the local conditions are the same for all stations. We can choose the reference value of amplitude at the station with hard bedrock. In our study, the station KHC was chosen as the reference station. The amplification factor is then computed as the ratio of the amplitude at the current station and at the reference station.

We have applied this method using 6 distant earthquakes (the same as in paragraph 4). For further analysis, we will use the compensated seismograms.

6. Attenuation of *PGV* and *PGA* with epicentral distance

The first step is the determination of mean decay of amplitudes with epicentral distance, (without considering azimuthal dependence) for each event. As the magnitudes of the events are not the same, we determine the parameters for the individual earthquakes.

We assume the dependence on the epicentral distance R in the form:

$$\log(PGA)(R) = \log(PGA)(100) - 0.5 \log(R/100) - \alpha \, (R/100-1)$$

$$\log(PGV)(R) = \log(PGV)(100) - 0.5 \log(R/100) - \beta \, (R/100-1) \qquad (2)$$

where $PGA(100)$ and $PGV(100)$ are the expected peak amplitudes for an earthquake in the epicentral distance of 100 km. The values are dependent on the magnitude, depth and other parameters of the particular earthquake. The second term in (2) characterizes the geometrical spreading of rays, and the third term represents material attenuation, α, β are constants.

The equations do not cover the amplitudes in epicentral areas up to the epicentral distance of 50 km where the amplitudes of seismic waves are strongly affected by focal mechanisms and by hypocentral depth. Moreover, *PGA* in such small epicentral areas contains high frequencies that cause a significant difference between the original and the filtered seismogram. Constant 0.5 in the second term in (2) represents the geometrical spreading of the rays. It is characteristic for surface waves and also for waves Pg, Pn, Sg, Sn, for which most of the energy remains in the Earth's crust. The third term represents amplitude attenuation of the plane wave, which is caused by inelasticity of the rock massif. We determine the attenuation separately for seismic velocity and acceleration. We used optimization to find the parameters that are summarized in Table 2 for *PGV* and Table 3 for *PGA*. We identified models both for vertical and horizontal components. The example of attenuation model of PGA_H for Earthquake 7 is shown in Figure 4a. Attenuation of all earthquakes and PGV_Z, PGV_H, PGA_Z, PGA_H are in Appendices 2 and 3.

ID	Date & time	Log(PGV$_Z$)(100)	Log(PGV$_H$)(100)	α_Z	α_H

		UTC	μm/s	μm/s	(100km)⁻¹	(100km)⁻¹
E1	2012-01-17 11:41:01.0		0.672	0.986	0.175	0.223
E2	2012-03-05 22:56:57.0		0.471	0.699	0.116	0.130
E3	2014-04-17 14:59:17.0		1.096	1.368	0.140	0.140
E4	2014-05-31 10:37:20.9		2.147	2.432	0.347	0.354
E5	2014-11-14 10:44:18.4		0.583	0.741	0.194	0.172
E6	2015-07-08 06:53:18.1		1.533	1.701	0.213	0.204
E7	2016-04-25 10:28:22.9		1.624	1.900	0.250	0.249
E8	2018-05-21 21:04:43.0		1.649	1.962	0.306	0.330
E9	2018-07-20 03:31:30.7		1.400	1.638	0.172	0.174

Table 2: Parameters of attenuation of *PGV* for earthquakes E1 to E9.

ID	Date & time	Log(PGA$_Z$)(100)	Log(PGA$_H$)(100)	β_Z	β_H
	UTC	mm/s²	mm/s²	(100km)⁻¹	(100km)⁻¹
E1	2012-01-17 11:41:01.0	-0.695	-0.461	0.234	0.320
E2	2012-03-05 22:56:57.0	-1.160	-0.944	0.132	0.165
E3	2014-04-17 14:59:17.0	-0.406	-0.287	0.181	0.164
E4	2014-05-31 10:37:20.9	0.790	0.996	0.487	0.512
E5	2014-11-14 10:44:18.4	-1.029	-1.067	0.208	0.194
E6	2015-07-08 06:53:18.1	-0.124	0.078	0.314	0.364
E7	2016-04-25 10:28:22.9	0.184	0.391	0.305	0.358
E8	2018-05-21 21:04:43.0	0.265	0.511	0.426	0.488
E9	2018-07-20 03:31:30.7	-0.284	-0.020	0.273	0.346

Table 3: Parameters of attenuation of *PGA* for earthquakes E1 to E9.
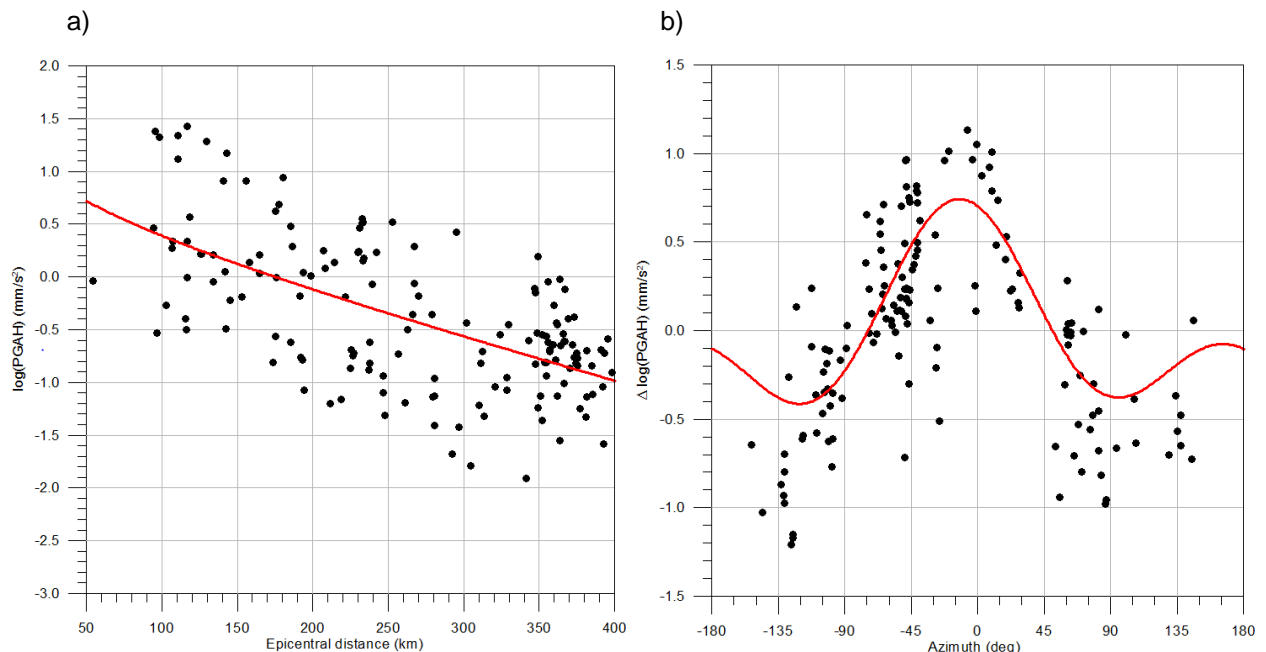
Figure 4: Attenuation of *PGA$_H$* for earthquakes E7, dependence a) on epicentral distance, b) on azimuth

$$f(\varphi) = 0.41 cos(\varphi + 10°) + 0.33 cos\big(2(\varphi - 13°)\big)$$

7. Azimuthal dependence of PGA and PGV

Azimuthal dependence of PGV and PGA attenuation is the main topic of this study. It was confirmed recently for the source zone of the Vienna Basin by Málek and Brokešová (2017). Now, we analyze this phenomenon for more source zones in the vicinity of the Bohemian Massif.

We consider the attenuation model (from Chap. 5 - dependent only on epicentral distance) as the mean model and analyze the differences (ratios of the peak amplitudes) from it. We compute the ratio of the measured value and the mean model and show it as a function of the azimuth (from the epicenter to the station). The example of azimuthal dependence of PGA_H for Earthquake 7 is shown in Figure 4b. The red line represents the best fit of the function:

$$f(\varphi) = A\cos(\varphi - \varphi_1) + B\cos\big(2(\varphi - \varphi_2)\big)$$

Where φ is the azimuth and A, B, φ_1, φ_2 are parameters determined by optimization.

Azimuthal dependence of all earthquakes and PGV_Z, PGV_H, PGA_Z, PGA_H are in Appendices 4 and 5. Their shape is different for different events. It is most pronounced for events E1, E2, E3 and E7. The azimuth of the strongest amplitude differs a little for these earthquakes, but generally it is to North. For earthquakes E4 and E8 (Nový Kostel, Czechia), no azimuthal dependence is observed. For other earthquakes (E5, E6, E9) (Mining rockburst at Lubin and Ostrava), the azimuthal distribution is not sufficient to make reliable conclusions.

The prevailing frequency of the maximum amplitudes F_M can be roughly estimated from the ratio of PGA and PGV, according formula (1). Its value is shown in map in Figures 5. The frequency does not correlate with epicentral distance and it is very different for various events (in the same epicentral distance). This indicates that in PSHA we cannot use the standard approach of universal spectra (dependent only on epicentral distance). To make a truly site-specific frequency model, we have to define the expected spectra for every source zone separately. Such task, however, requires more data. We have to wait for more future earthquakes that can be analyzed.
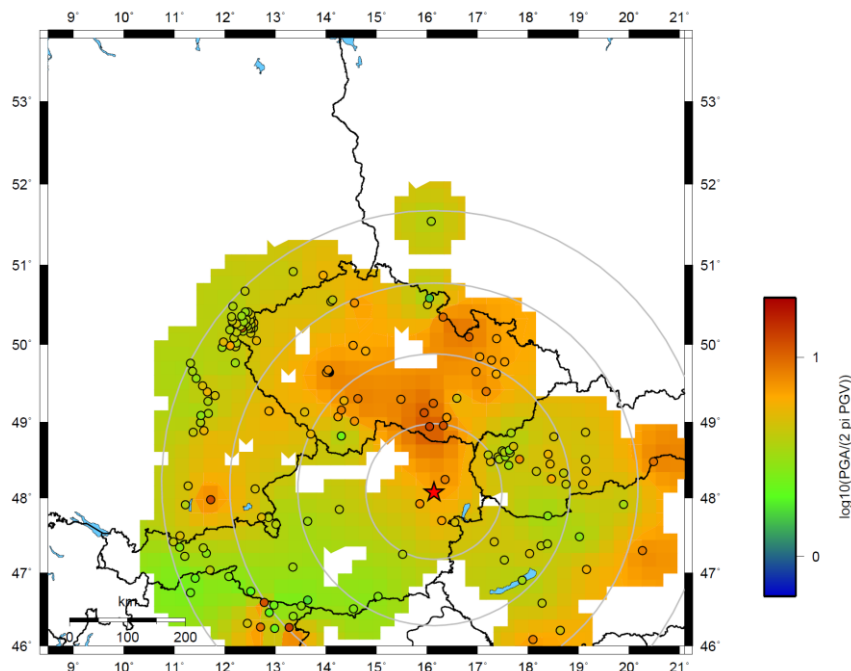

Figure 5: Frequency F_M. Circles denote epicentral distances of 100, 200, 300 and 400 km.

8. Discussion

The explanation of the observed azimuthal dependence of the peak amplitudes at the earthquakes E1, E2, E3 and E7 is not clear yet. It cannot be fully explained by radiation patterns of the earthquakes. For all of these earthquakes, we can see only one maximum and one minimum in the azimuth dependence, which does not fit the expected radiation pattern from a double-couple source (two maxima and two minima). The directivity of the source radiation cannot explain it either, because the maximum azimuth does not fit the strikes of the faults. The azimuth of the maximum amplitudes is approximately North for all of the earthquakes. Therefore, we prefer the hypotheses that the azimuthal dependence is mainly a consequence of the complex geological structure in the region, which can focus the seismic energy in North direction. The differences in prevailing frequency (Fig.5) and the differences of parameters α, β, (see Tables 3,4) seem to prove that also the material attenuation is very different for various geological structures in the region and that it has an important impact on the frequency content and the peak amplitudes.

The most significant problem during our study was the lack of data. There are not enough regional earthquakes recorded at a sufficient number of stations. There is a good chance that more data will be available in the near future. The number of stations installed in the Bohemian Massif is now much higher than in the past, so every new regional earthquake will improve our set of events used.

9. Conclusion

A truly site-specific PSHA requires GMMs derived with the help of seismograms measured in the same region for which the PSHA is performed. This principle is especially important in a situation where the controlling earthquakes (which are responsible for seismic hazard) are situated far away from the site. Such situation is typical for the nuclear power plants of Temelín and Dukovany in the Bohemian Massif. The disaggregation of seismic hazard has shown that the most important source zones are situated in the Alps and in West Bohemia, more than one hundred kilometers from the sites. The local seismicity near power plants is very weak. We used moderate-size earthquakes that occurred from 2012 to 2018 to show that in epicentral distances over 50 km, amplitudes of seismic waves from some earthquakes are strongly dependent on the azimuth of the wave propagation. The mean model (dependent only on epicentral distance) differs more than 10 times from the amplitudes measured at some stations. If we use only the mean model not taking into account the azimuth (which is a standard approach in PSHA), we have to introduce substantive uncertainties. The model that includes the azimuthal term is much more precise. Its incorporation into the PSHA requires a modification of the standard methodology, as we have to introduce an individual, azimuth-dependent attenuation model for each source zone.

References

Málek J., Brokešová J., and Vackář J., (2017): Mid-European seismic attenuation anomaly. *Tectonophysics* 712-713, 557-577, DOI: 10.1016/j.tecto.2017.06.003

Málek J., Prachař I., Šílený J., Gaždová, R., (2012): Assessment of the SL-2 value for Temelín and Dukovany NPPs. ČEZ a.s., internal report.

Málek J., Prachař I. (2015): Probabilistic Seismic Hazard Assessment of the Dukovany Nuclear Power Plant. ČEZ a.s., internal report.

Christine A. Goulet, Yousef Bozorgnia, Nicolas Kuehn, Linda Al Atik, Robert R. Youngs, Robert W. Graves, and Gail M. Atkinson (2017): NGA-East Ground-Motion Models for the U.S. Geological Survey National Seismic Hazard Maps. PEER 2017/03. Pacific Earthquake Engineering Research Center

Zátopek, A., 1948. The Propagation of East Alpine Earthquakes in the Bohemian Mass, Publications De l'Institut Geophysique National, Tchécoslovaquie, Travaux Speciaux, No.3.

List of appendices